Topological Characterization of *Escherichia coli* DMSO Reductase by Electron Paramagnetic Resonance Spectroscopy of an Engineered [3Fe–4S] Cluster†

Richard A. Rothery and Joel H. Weiner*

Department of Biochemistry, 474 Medical Sciences Building, University of Alberta, Edmonton, Alberta, Canada T6G 2H7

Received September 21, 1992; Revised Manuscript Received March 19, 1993

ABSTRACT: We have applied the technique of distance estimations using the exogenous paramagnetic probe dysprosium(III) complexed with EDTA (DyEDTA) to study the topology of *Escherichia coli* dimethyl sulfoxide reductase (DmsABC) *in situ* in cytoplasmic membrane and whole cell preparations. The electron transfer subunit (DmsB) of this enzyme contains four [4Fe–4S] clusters and has complex EPR properties making it unsuitable for studies utilizing exogenous paramagnetic probes. We have utilized a mutant of DmsABC in which one of the [4Fe–4S] clusters of DmsB has been changed to a [3Fe–4S] cluster [Rothery, R. A., & Weiner, J. H. (1991) *Biochemistry 30,* 8296–8305]. This mutant (DmsB-C102S) has a single magnetically isolated EPR visible [3Fe–4S] cluster in its fully oxidized state, making it suitable for studies using DyEDTA as paramagnetic probe. We have studied the effect of DyEDTA on the microwave power saturation properties of the EPR signal of the DmsB-C102S mutant. DyEDTA enhances the spin relaxation of the [3Fe–4S] signal in everted membrane vesicles. It has a smaller effect on the spin relaxation of the [3Fe–4S] signal in whole cell preparations. We conclude that the [3Fe–4S] cluster of the DmsB-C102S mutant is located on the inside of the cytoplasmic membrane. We have estimated the distance of this center from the surface of the DmsAB dimer to be approximately 21 Å, close to the cytoplasmic-side membrane surface level, by calibrating the DyEDTA effect using a myoglobin nitroxide standard.

Escherichia coli, when grown anaerobically with dimethyl sulfoxide (DMSO)[1] as respiratory oxidant, develops a respiratory chain terminated by a membrane-bound menaquinol: DMSO oxidoreductase (DMSO reductase, DmsABC; Weiner et al., 1992). This enzyme is a heterotrimer comprising a molybdopterin (Moco)-containing catalytic subunit (DmsA, 87.4 kDa), an [Fe–S] cluster containing electron-transfer subunit (DmsB, 23.1 kDa), and a membrane anchor subunit (DmsC, 30.8 kDa; Bilous et al., 1988). DmsABC can be readily overexpressed from plasmids bearing the *dmsABC* operon, and the overexpressed enzyme assembles normally into the cytoplasmic membrane (Weiner et al., 1988; Cammack & Weiner, 1990). The catalytic and electron transfer subunits are also found as a soluble DmsAB dimer which accumulates in the cytoplasm of cells overexpressing DmsABC (Bilous & Weiner, 1988; Cammack & Weiner, 1990). DmsABC is a good model system for a group of trimeric iron–sulfur molybdoenzymes including *E. coli* formate dehydrogenase (FdnGHI; Berg et al., 1991) and *E. coli* nitrate reductases (NarGHJI and NarZYWV; Blasco et al., 1989, 1990).

Sambasivarao et al. (1990) studied the topology of DmsABC using a variety of biochemical techniques. These workers concluded that the DmsAB dimer is anchored to the inner side of the cytoplasmic membrane by DmsC. This topology bears interesting comparison with that found for *E. coli* TMAO reductase and the DMSO reductases from a range of bacteria (Weiner et al., 1992). These enzymes are typically soluble, periplasmically localized, and accept electrons from cytochromes rather than from menaquinol. It would be interesting to compare the topology of DmsABC derived from biochemical studies (Sambasivarao et al., 1990) with data obtained from an alternative biophysical technique.

Gadolinium(III) and dysprosium(III) have been used as effective paramagnetic probes in a number of proteins containing electron paramagnetic resonance (EPR) visible species. These include the photoreaction center of PSII in *Rhodobacter sphaeroides* (Innes & Brudvig, 1989), the bovine cytochrome bc_1 complex (Ohnishi et al., 1989), and *Rhodobacter capsulatus* cytochrome bc_1 (Meinhardt & Ohnishi, 1992). These probes are most effective in systems where there are magnetically isolated paramagnetic species present in the protein being studied. In this respect DmsABC is unsuitable, as there are four [4Fe–4S] clusters present, all of which are paramagnetic in the fully reduced enzyme with considerable signal overlap. In addition, the four centers are partially spin coupled (Cammack & Weiner, 1990). We recently showed that it is possible to change one of the [4Fe–4S] clusters of DmsB to a [3Fe–4S] cluster by site-directed mutagenesis (Rothery & Weiner, 1991). This genetically engineered center is the only paramagnetic species present in the fully oxidized enzyme, and this makes it amenable to studies utilizing paramagnetic probes.

The effect of paramagnetic probes on the spin relaxation times of various EPR visible prosthetic groups has been used to estimate distances between the endogenous paramagnetic centers and their respective protein surfaces. Ohnishi and co-workers (Blum et al., 1980, 1981, 1983) developed empirical methods to estimate distances between the surface of globular proteins and intrinsic paramagnetic centers using dysprosium-(III) as a paramagnetic probe. More recently (Innes & Brudvig, 1989; Meinhardt & Ohnishi; 1992), this technique has been extended to study the topology of membrane proteins. The method is of low resolution but can provide new topological insights where other data (i.e., crystal structures) are unavailable. We have previously shown (Rothery & Weiner, 1991) that the DmsB-C102S mutant DmsABC does not

† This work has funded by a grant from the Medical Research Council of Canada to J.H.W. (PG11440). R.A.R. was a postdoctoral fellow of the Alberta Heritage Foundation for Medical Research.

* Author to whom correspondence should be addressed.

[1] Abbreviations: DmsABC, DMSO reductase; DMSO, dimethyl sulfoxide; EPR, electron paramagnetic resonance spectroscopy; GF, glycerol–fumarate minimal medium; MbNO, myoglobin nitroxide; Moco, molybdopterin cofactor; TMAO, trimethylamine-*N*-oxide.

0006-2960/93/0432-5855$04.00/0

support menaquinol:DMSO oxidoreductase activity. This suggests that the [4Fe–4S] cluster to which DmsB-C102 provides a ligand is important in electron transfer from menaquinol to Moco in DmsA. It would therefore be interesting to use the paramagnetic probe technique to estimate how close the mutant [3Fe–4S] cluster is to the protein surface. Such studies will help determine the function of the corresponding [4Fe–4S] cluster of the wild-type enzyme in DMSO reduction.

In this paper, we have used dysprosium-EDTA (–1) as a paramagnetic probe to determine the membrane sidedness of the DmsB electron transfer subunit of *E. coli* DMSO reductase and have obtained a low-resolution estimate of the distance of the DmsB–C102S mutant [3Fe–4S] cluster below the surface of the protein.

MATERIALS AND METHODS

Growth of Cells. *E. coli* HB101 (*supE*44 *hsdS*20($r_B^-m_B^-$) *rec*A13 *ara*-14 *pro*A2 *lacY*1 *galK*2 *rpsL*20 *xyl*-5 *mtl*-1) was used throughout. HB101 was transformed with the plasmids pDMS160, pDMS160-C102S (Rothery & Weiner, 1991), and pBR322. pDMS160 encodes wild-type DmsABC, whereas pDMS160-C102S encodes a DmsB-C102S mutant containing a [3Fe–4S] cluster substituted for one of the [4Fe–4S] clusters of DmsB. pBR322 is the cloning vector used to construct pDMS160 and pDMS160-C102S. Cells were grown for 48 h anaerobically at 37 °C on a glycerol–fumarate minimal medium (GF) in the presence of 100 μg mL^{-1} ampicillin (Condon & Weiner, 1988) in 10- or 20-L batches at 37 °C. Under these growth conditions, plasmid-encoded DmsABC is the major EPR detectable species present in the cells (Rothery & Weiner, 1991; Cammack & Weiner, 1990). Cells were harvested by concentration using a Millipore Pellicon filter and centrifugation and were washed by resuspension in an appropriate buffer (see below) and recentrifugation.

Preparation of Membrane Vesicles. Cells were harvested, washed, and membranes prepared by French pressure cell lysis and differential centrifugation (Rothery & Weiner, 1991) in 50 mM MOPS, 70 mM TMAO, and 5 mM EDTA (pH 7.0). The buffer used during the French pressing step contained 0.2 mM PMSF. Prior to preparation of EPR samples, the buffer was exchanged for 100 mM MOPS and 5 mM EDTA (pH 7.0).

Preparation of Whole Cells. (*i*) *Outer Membrane Permeabilized Cells.* These were prepared as described by Lin and Cheng (1991). Cells grown on 10 L of GF (8 g, wet weight) were harvested, washed in 100 mM MOPS and 5 mM EDTA (pH 7.0), and resuspended in 500 mL of 20 mM Tris, 20% (w/v) sucrose, and 1 mM EDTA. Following incubation on ice for 10 min, 250 mL of this cell suspension was pelleted by centrifugation at 4000*g* for 10 min and resuspended carefully in 250 mL of ice-cold water. The cells were incubated for a further 10 min on ice, centrifuged at 8000*g* for 10 min, and carefully resuspended in 50 mM MOPS and 5 mM EDTA.

(*ii*) *Whole Cells.* Cells were grown in 10-L batch culture on GF, harvested as above, and then washed in 100 mM MOPS and 5 mM EDTA (pH 7.0) and carefully resuspended in 100 mM MOPS and 5 mM EDTA (pH 7.0).

Preparation of Cytoplasmic Fractions. Cytoplasmic fractions were obtained as the supernatant following centrifugation of French pressure cell lysates at 150000*g* for 1.5 h. The buffer used throughout was 100 mM MOPS and 5 mM EDTA (pH 7.0). PMSF (0.2 mM) was added to this buffer prior to cell lysis.

Preparation of DyEDTA and LaEDTA. We used DyEDTA (–1) as a paramagnetic probe. Other chelators for Dy^{3+} are available (Ohnishi et al., 1985), but the use of EDTA has been shown to produce reliable results in studies of a number of electron transfer chain complexes (Meinhardt & Ohnishi, 1992; Innes & Brudvig, 1989). $DyCl_3$ or $LaCl_3$ (Sigma) were chelated with EDTA in a 1:1 molar ratio, and the pH was brought to 7.0 (Blum et al., 1983).

Preparation of EPR Samples. Membrane or whole cell preparations were used to prepare EPR samples in the presence of 0–10 mM DyEDTA. Membrane samples were oxidized with 0.15 mM ferricyanide. Whole cell samples were oxidized with 1–5 mM ferricyanide. Cytoplasmic fractions were oxidized with 5 mM ferricyanide. Samples were rapidly frozen in a dry ice–ethanol mixture before being stored under liquid N_2 at 77 K. Reduced samples were prepared by reduction with 5 mM dithionite for 1 min (Rothery & Weiner, 1991). Myoglobin nitroxide (MbNO) samples were prepared as follows: 1-mL aliquots of a 10 mg mL^{-1} solution of Mb in 100 mM MOPS, 50 mM sodium nitrite, 5 mM EDTA (pH 7.0), and 0–10 mM DyEDTA were reduced with a few grains of sodium dithionite for 1 min and were transferred to EPR tubes, frozen, and stored as described above.

EPR Spectroscopy. EPR spectra were recorded using a Bruker Spectrospin ESP-300 spectrometer equipped with an Oxford Instruments ESR-9 flowing helium cryostat. Instrument conditions and temperature conditions were as described in the individual figure legends. Microwave power saturation data were plotted and fitted to an empirical equation as described by Rupp et al. (1978). Microwave power saturation data were fitted to $S = K\sqrt{P}/(1 + P/P_{1/2})^{0.5b}$, where S is the signal height, K is a proportionality factor, P is the microwave power, $P_{1/2}$ is the power for half saturation, and b is the inhomogeneity parameter (Innes & Brudvig, 1989).

RESULTS

Microwave Power Saturation of Wild-Type and DmsB-C102S DMSO Reductase. Figure 1 shows EPR spectra of dithionite-reduced and ferricyanide-oxidized HB101 membranes containing overexpressed wild-type and DmsB-C102S DMSO reductase. Figure 2 shows the corresponding microwave power saturation curves recorded at 10 K. The signal of oxidized DmsB-C102S DMSO reductase is readily saturated at 10 K, with a $P_{1/2}$ of 6.5 mW. The $P_{1/2}$ of the C102S [3Fe–4S] signal has a T^9 temperature dependence between 8 and 14 K, indicative of a second-order Raman relaxation mechanism (data not shown; Blum et al., 1983). The EPR signals of reduced wild-type and DmsB-C102S DMSO reductases are not readily saturable with increasing microwave power, and this result is consistent with the studies of Rupp et al. (1978), who found that the signals from fully reduced eight-iron ferredoxins are more difficult to saturate than singly reduced ferredoxins. Because of the rapid spin relaxation of dithionite-reduced wild-type and DmsB-C102S DMSO reductases, we decided to study the effect DyEDTA on the oxidized signal of the DmsB-C102S mutant. The oxidized [3Fe–4S] cluster of this enzyme is magnetically isolated in the redox range in which it is oxidized (>150 mV; Rothery & Weiner, 1991) and therefore can be studied in the absence of interactions with other paramagnetic species within the enzyme. The DmsB-C102S mutant was chosen for the studies described herein because the spectrum of the [3Fe–4S] cluster it contains is readily saturable between 8 and 12 K and the oxidized cluster is a magnetically isolated single-spin species (Rothery & Weiner, 1991).

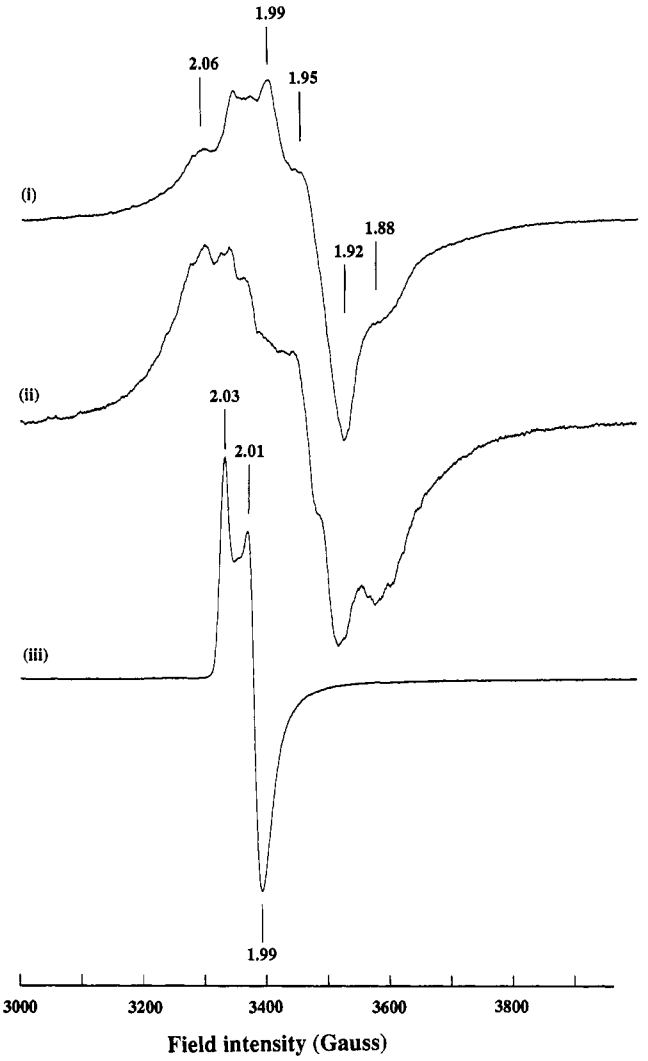

FIGURE 1: EPR spectra at 12 K of DmsABC in HB101 cytoplasmic membranes. (i) Dithionite-reduced wild-type (HB101/pDMS160); (ii) dithionite-reduced DmsB-C102S (HB101/pDMS160-C102S); and (iii) ferricyanide-oxidized DmsB-C102S. Samples were prepared by reduction with 5 mM sodium dithionite for 1 min or oxidation with 0.15 mM potassium ferricyanide. EPR instrument conditions: microwave power, 20 mW; microwave frequency, 9.45 GHz; modulation amplitude, 10 G_{pp} at 100 kHz.

Effect of DyEDTA on the EPR Spectrum of Oxidized DmsB-C102S Membranes. Figure 3 shows EPR spectra recorded at 12 K of DmsB-C102S membranes. Addition of DyEDTA results in a broadening of the EPR spectrum, with the $g = 2.01$ peak being lost at higher concentrations. This effect is also seen in the whole cell preparations used in this work (data not shown). The effect of DyEDTA on the line width of an intrinsic center is effective over a greater distance than its effect on the spin relaxation of the intrinsic center (an r^{-3} versus an r^{-4} to r^{-6} distance dependence; Blum et al., 1981; Ohnishi et al., 1989). For this reason, we were unable to assign the membrane sidedness of the [3Fe–4S] cluster of the DmsB-C102S mutant from the line-broadening effect.

Effect of DyEDTA on the $P_{1/2}$ of the [3Fe–4S] Center in Membranes. Figure 4 shows the effect of increasing concentrations of DyEDTA on microwave power saturation curves of the [3Fe–4S] signal from the DmsB-C102S mutant of DMSO reductase. DyEDTA causes the $P_{1/2}$ of the [3Fe–4S] signal to be increased at 8, 10, and 12 K. At each temperature, the data can readily be fitted to a single species according to the method of Rupp et al. (1978). $\Delta P_{1/2}$ values (Blum et al., 1981, 1983) obtained from plots of $P_{1/2}$ versus probe concentration are 0.85, 3.47, and 9.41 mW mM^{-1}, at 8, 10,

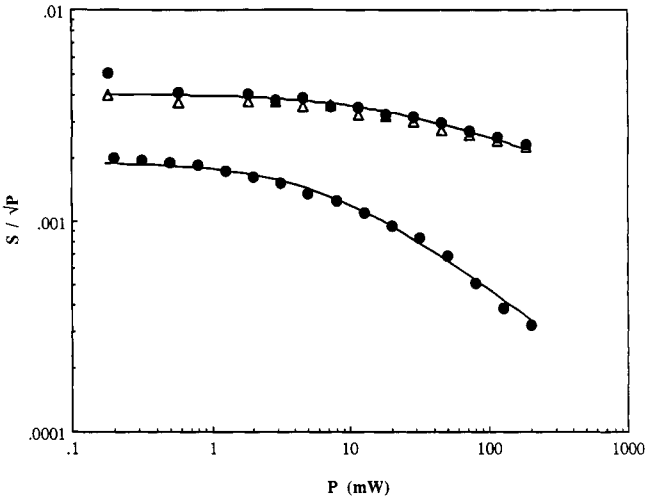

FIGURE 2: Microwave power saturation profiles of reduced wild-type DMSO reductase and reduced and oxidized DmsB-C102 DMSO reductase at 10 K. (△) Reduced wild-type enzyme, saturation of the $g = 1.92$ trough (Figure 1); (●) reduced (upper, saturation of the $g = 1.92$ trough) and oxidized (lower, saturation of the $g = 2.03$ peak) DmsB-C102S DMSO reductase. The reduced signals could not be fitted to the empirical equation (see Materials and Methods). The oxidized DmsB-C102S signal was fitted to a $P_{1/2}$ of 6.5 mW, $b = 1.0$.

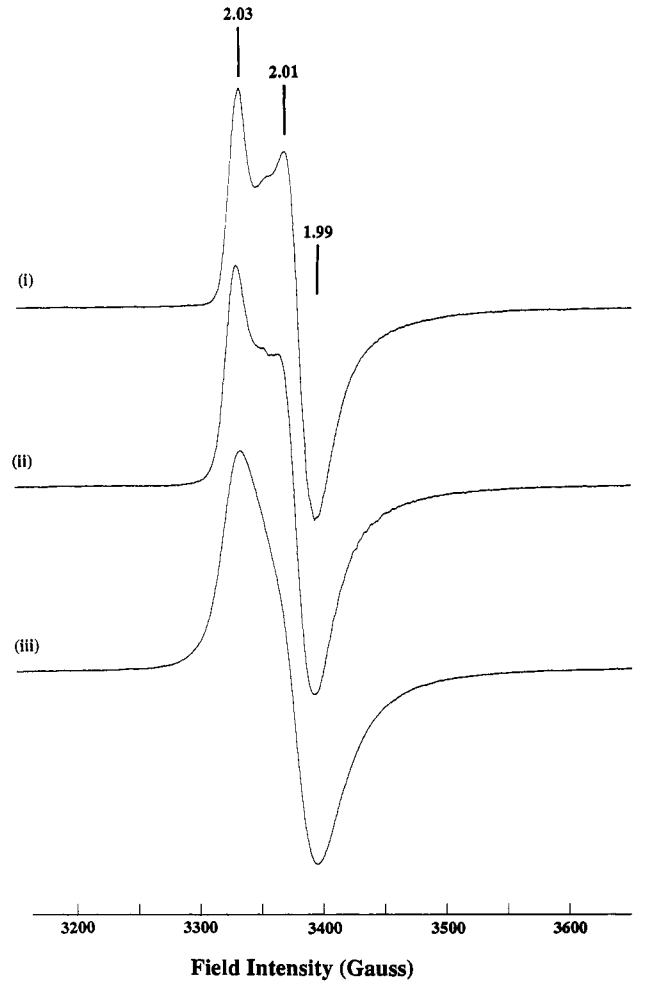

FIGURE 3: EPR spectra of the DmsB-C102 mutant [3Fe–4S] cluster in membranes at 12 K in the presence of increasing concentrations of DyEDTA: (i) 0 mM; (ii) 2 mM; and (iii) 10 mM. Spectra were recorded using the conditions of Figure 1.

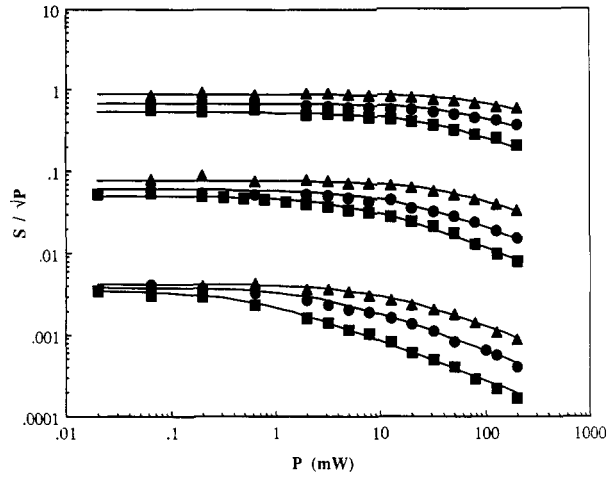

FIGURE 4: Microwave power saturation curves of membranes containing DmsB-C102S DMSO reductase at 12 (top), 10 (middle), and 8 K (bottom): (■) 0 mM; (●) 2 mM; and (▲) 10 mM DyEDTA. Data were fitted to the empirical equation with $b = 1.0$.

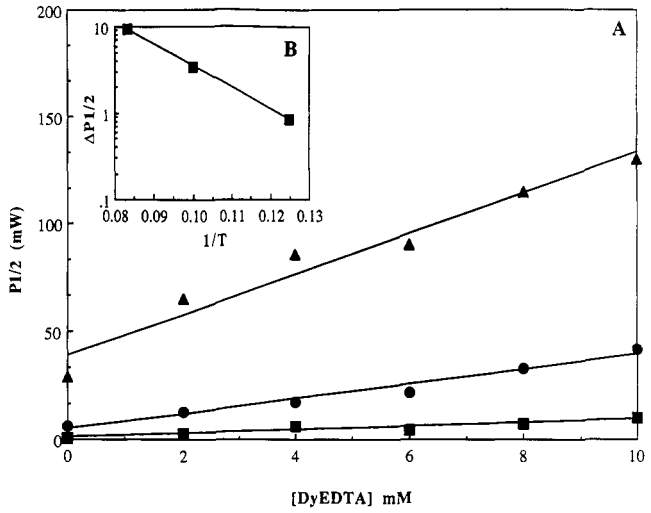

FIGURE 5: (A) Concentration dependence the $P_{1/2}$ on DyEDTA concentration at 8 (■), 10 (●), and 12 K (▲). $\Delta P_{1/2}$ values for each temperature were 0.85, 3.47, and 9.41 mW mM^{-1}, respectively. (B) Effect of temperature on the $\Delta P_{1/2}$.

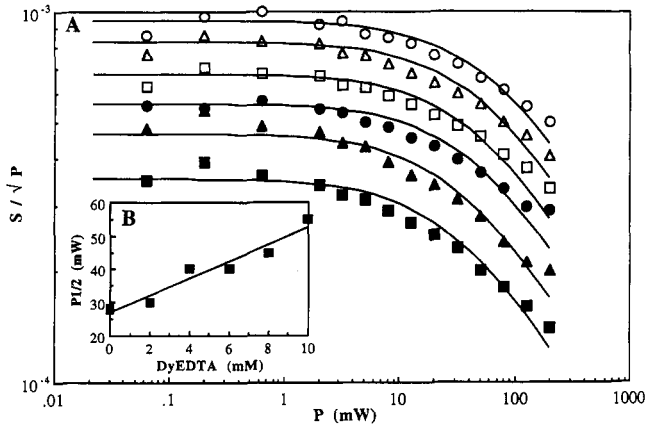

FIGURE 6: (A) Microwave power saturation curves of outer membrane permeabilized whole cells in the presence of 0 (■), 2 (▲), 4 (●), 6 (□), 8 (△), and 10 (○) mM DyEDTA. (B) DyEDTA concentration dependence of the $P_{1/2}$. Data were fitted to the empirical equation with $b = 1.0$. The $\Delta P_{1/2}$ was estimated to be 2.57 mW mM^{-1}.

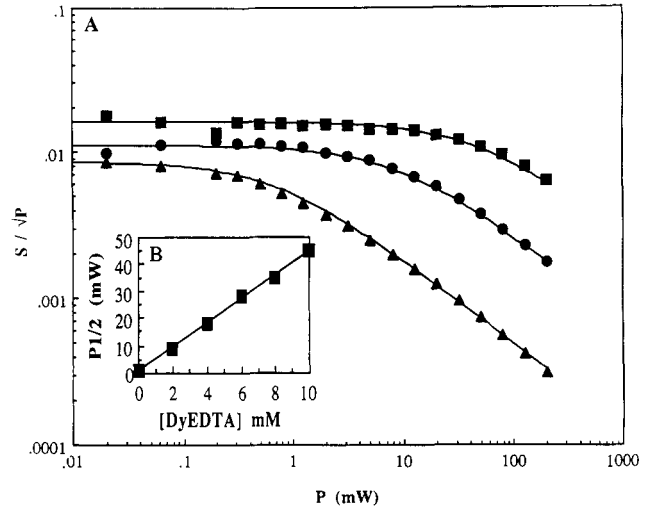

FIGURE 7: (A) Microwave power saturation curves of MbNO at 12 K in the presence of 0 (▲), 2 (●), and 10 mM (■) DyEDTA. The data were fitted to the empirical equation with $b = 1.15$. (B) DyEDTA concentration dependence of the $P_{1/2}$. The data could be fitted to a concentration dependence $\Delta P_{1/2}$ of 4.44 mW mM^{-1}.

and 12 K, respectively (Figure 5A). These values can be used to obtain low-resolution estimates of the distance from the surface of the protein to the [3Fe–4S] cluster (see below). Figure 5B shows the effect of temperature on the $\Delta P_{1/2}$, indicating that $\Delta P_{1/2} \propto \exp(-57/T)$. The diamagnetic control complex, LaEDTA, had no effect on the $P_{1/2}$ or the line shape of the [3Fe–4S] signal (data not shown).

Effect of DyEDTA on the $P_{1/2}$ of the [3Fe–4S] Center in Whole Cells. In order to determine the sidedness of DmsB with respect to the cytoplasmic membrane, we studied the effect of DyEDTA on the microwave power saturation properties of the [3Fe–4S] cluster of the DmsB-C102S mutant in whole cells and outer membrane permeabilized cells. The DyEDTA complex should be freely diffusable into the periplasmic space, as its molecular mass (0.431 kDa) is below the porin cutoff of 0.6 kDa (Nikaido & Vaara, 1987). Figure 6A shows a series of power saturation curves obtained from outer membrane permeabilized cells at 12 K. Similar results were obtained with whole cells, indicating that the intact outer membrane is permeable to the DyEDTA complex. It is more difficult to fit the microwave power saturation data of the outer membrane permeabilized cells to the empirical equation of Rupp et al. (1978) than is the case with membrane samples (cf. Figure 6A and Figure 4). Figure 6B shows the effect of increasing DyEDTA concentration on the $P_{1/2}$. The $\Delta P_{1/2}$ in this case is estimated to be 2.57 mW mM^{-1} (Figure 6B).

Effect of DyEDTA on the $P_{1/2}$ of MbNO. In order to estimate the distance of the [3Fe–4S] cluster below the surface of the DmsB-C102S DMSO reductase, we calibrated the DyEDTA effect using MbNO (Blum et al., 1983; Innes & Brudvig, 1989). Figure 7A shows the effect of DyEDTA on saturation profiles of the $g = 1.98$ trough of the MbNO signal at 12 K. The EPR spectrum of MbNO is a composite of two species (Trittelvitz et al., 1972; Hori et al., 1981) which have different g values and temperature dependencies. However, the data of Figure 7A indicate that the $g = 1.98$ feature of the MbNO EPR spectrum saturates as a single species with increasing microwave power. DyEDTA increased the $P_{1/2}$ with a $\Delta P_{1/2}$ of 4.44 mW mM^{-1} at 12 K (Figure 7B).

Estimation of the Distance of the [3Fe–4S] Cluster below the DyEDTA-Accesible Surface of Membrane Vesicles and Outer Membrane Permeabilized Cells. We have applied the methodology of Blum et al. (1983) and Ohnishi et al. (1989) to estimate effective distances using DyEDTA as a paramagnetic probe. In this method, the $\Delta P_{1/2}$ is compared to data obtained using a distance standard (MbNO) using an

Table I: Distance of the DmsB-C102S [3Fe-4S] from the Protein Surface

sample	$\Delta P_{1/2}$[a] (mW mM^{-1})	$\Delta P_{1/2,N}$[b] (mM^{-1})	effective distance k_{MO} (Å)[c]	effective distance k_{BO} (Å)[d]
MbNO	4.44	6.35		11.4[e]
[3Fe-4S] membranes	9.41	0.33	21.1	9.0
[3Fe-4S] cells	2.57	0.09	42.2	13.8

[a] $\Delta P_{1/2}$ obtained from plots of $P_{1/2}$ versus DyEDTA concentration. [b] $\Delta P_{1/2,N} = \Delta(P_{1/2,i}/P_{1/2,0})/\Delta$[DyEDTA]; where $P_{1/2,i} = P_{1/2}$ when [DyEDTA] = i mM; $P_{1/2,0} = P_{1/2}$ when [DyEDTA] = 0 mM. $\Delta P_{1/2,N}$ is the normalized $\Delta P_{1/2}$ as described by Meinhardt and Ohnishi (1992). [c] $k_{MO} = (\Delta P_{1/2,N,MbNO}/\Delta P_{1/2,N,FeS})^{1/x}(R_{std} + 5) - 5$, using normalized $\Delta P_{1/2}$'s as described by as described by Meinhardt and Ohnishi (1992). $\Delta P_{1/2,N}$ in membranes was multiplied by $^6/_5$ to account for the inaccessibility of the DmsAB/DmsC interface region to the DyEDTA probe (see text). $x = 6$ in membranes and 4 in whole cells. [d] k_{BO} was calculated as for k_{MO}, but nonnormalized $\Delta P_{1/2}$ values were used (Blum et al., 1983). $\Delta P_{1/2,FeS}$ was multiplied by $^6/_5$ as above in membranes. [e] Standard effective radius obtained from crystallographic data (Blum et al., 1983).

empirical equation: $k_i = (\Delta P_{1/2,std}/\Delta P_{1/2,i})^{1/x}(k_{std} + 5) - 5$, where k_i = effective radius of the protein under study; k_{std} = effective radius of the standard used (MbNO, 11.4 Å; Blum et al., 1983); $\Delta P_{1/2,std} = \Delta P_{1/2}$ of the standard; $\Delta P_{1/2,i} = \Delta P_{1/2}$ of the protein under study; 5 = radius of the DyEDTA complex (Å); and x = the distance dependence of the DyEDTA effect, where $x = 4$ for centers under a DyEDTA-accesible plane (Ohnishi et al., 1989), and $x = 6$ for centers under a DyEDTA-accessible sphere (Blum et al., 1983). In all our estimations of $P_{1/2}$ values of the DmsB-C102S [3Fe–4S] signals, we used an inhomogeneity parameter (b) of 1.0. Estimations of the $P_{1/2}$ values of the MbNO signals were performed using an inhomogeneity parameter of 1.15. In both cases, other values for b produced poor fits to the data. Meinhardt and Ohnishi (1992) studied the $Q_i^{\bullet-}$ radical binding site of complex III of *R. capsulatus* using fatty-acid-bound spin labels as distance standards and found that the most reliable distance estimations are based on calculations using normalized $\Delta P_{1/2}$ ($\Delta P_{1/2,N}$; see footnote of Table I). Such an analysis compensates for differences in the intrinsic spin–lattice relaxation times (T_1) between the distance standards and the paramagnetic center being studied. In our work, the standard used is a soluble protein, whereas the DmsB-C102S [3Fe–4S] center is within the membrane extrinsic DmsAB dimer. The DmsAB dimer has been visualized as an approximately 50-Å diameter spheroid attached to the surface of the membrane (Weiner et al., 1992), and we have made the assumption that approximately $^1/_6$ of its surface area is not accessible to the DyEDTA probe (this value is based on the analogy of a cube resting on the membrane plane). To account for this we have multiplied the $\Delta P_{1/2}$ and $\Delta P_{1/2,N}$ values in membrane preparations by $^6/_5$. Using this technique, we can estimate the effective distance of the [3Fe–4S] cluster below the surface of the protein as being 21 Å (Table I). For comparison, a similar calculation using nonnormalized $\Delta P_{1/2}$ values gives a distance of 9.0 Å. In outer membrane permeabilized cells, the situation is different, with the periplasmic surface of DmsC exposed to DyEDTA, as well as the whole of the periplasmic surface of the cytoplasmic membrane. The calculation in this case assumes an r^{-4} dependence and yields a distance estimate of 42.2 Å using the normalized $\Delta P_{1/2}$ and 13.8 Å using the nonnormalized $\Delta P_{1/2}$.

Because of the weighted ($r^{-4} - r^{-6}$) averaging, the effective distance calculated is dominated by the relaxation enhancement effect by the spin probes at the closest approach. Therefore, the effective distance is somewhat longer than the shortest distance from the [3Fe–4S] cluster to the surface barrier.

EPR Characterization of Cytoplasmic Fractions Containing the Wild-Type and Mutant Soluble DmsAB Dimer. In order to explore the possibility of analyzing the topographical location of the [3Fe–4S] cluster in the soluble DmsAB-C102S dimer using the dysprosium probe technique, we recorded EPR spectra of cytoplasmic fractions from cells overexpressing mutant and wild-type DmsABC. Such cells have been shown to accumulate a soluble cytoplasmic DmsAB dimer (Bilous & Weiner, 1988; Cammack & Weiner, 1990; J. L. Simala and J. H. Weiner, unpublished results). Figure 8 shows spectra at 12 K of oxidized and reduced cytoplasmic fractions from HB101/pBR322, HB101/pDMS160, and HB101/pDMS160-C102S. Figure 8A shows spectra of ferricyanide-oxidized samples; each of these spectra has a near isotropic signal with a peak at $g = 2.02$, indicating the presence of [3Fe–4S] clusters. Surprisingly, the spectrum of the DmsB-C102S dimer in cytoplasmic fractions shows no evidence of the EPR-detectable [3Fe–4S] cluster found in membranes from HB101/pDMS160-C102S, and there appears to be little difference in the intensities of the oxidized spectra in the three strains studied. Figure 8B shows spectra of dithionite-reduced samples. These spectra clearly show that the soluble DmsAB dimer and DmsAB-C102S dimers have a [4Fe–4S] cluster composition very similar to that found in the respective membrane-bound holoenzymes [*cf.* Figure 8B (ii and iii) and Figure 1 (i and ii)]. These data indicate that in the DmsB-C102S enzyme the mutant [3Fe–4S] cluster is readily modified in the soluble DmsAB-C102S dimer.

DISCUSSION

The results reported herein indicate that the [3Fe–4S] cluster of the DmsB-C102S dimer can be readily studied using a combination of paramagnetic probes and EPR spectroscopy. The spin relaxation enhancement of the DyEDTA probe is much greater in membranes than in whole cells ($\Delta P_{1/2,membranes}$:$\Delta P_{1/2,cells}$ is approximately 9.41:2.57 mW mM^{-1} at 12 K). This indicates that the [3Fe–4S] cluster of the mutant protein is located on the inside of the cytoplasmic membrane. By extrapolation, we conclude that the DmsB subunit of the wild-type enzyme is also located on the inside of the cytoplasmic membrane.

We have previously shown (Rothery & Weiner, 1991) that changing the [4Fe–4S] cluster to which DmsB-C102 provides a ligand to a [3Fe–4S] cluster by site-directed mutagenesis results in an enzyme unable to support menaquinol:DMSO oxidoreductase activity. We have attempted to determine the position of the [3Fe–4S] cluster in the DmsB-C102S DmsAB dimer relative to the surface of the protein. Electron microscopy and immunological studies (Sambasivarao et al., 1990; Weiner et al., 1992) have already shown that DmsA and DmsB are arranged as an approximately 50-Å diameter dimer which is anchored to the membrane by the DmsC membrane intrinsic subunit. We have extended these studies using the paramagnetic probe technique to estimate the distance of the DmsB-C102S [3Fe–4S] cluster below the surface of the protein.

Paramagnetic lanthanides have been used in combination with EPR to estimate distances in a number of proteins (Blum et al., 1981, 1983; Ohnishi et al., 1989; Meinhardt & Ohnishi, 1992; Innes & Brudvig, 1989). These distance estimations have been based on manipulations of the $\Delta P_{1/2}$ parameters in relation to the $\Delta P_{1/2}$ of a protein of known structure, where the effective distance between the surface of the protein and

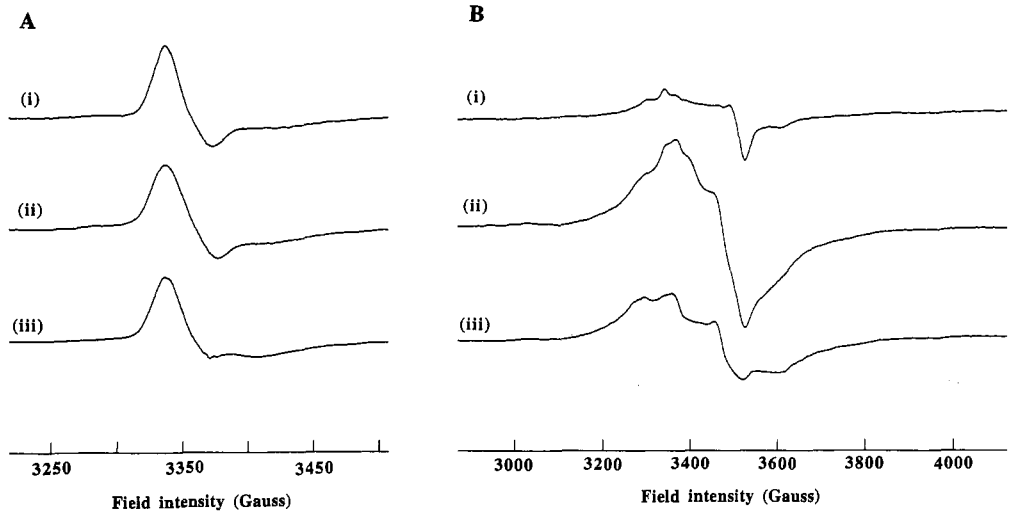

FIGURE 8: EPR spectra at 12 K of DmsAB in HB101 cytoplasmic fractions. (A) Ferricyanide (5 mM)-oxidized samples; (i) HB101/pBR322, (ii) HB102/pDMS160, and (iii) HB101/pDMS160-C102S. (B) Dithionite (5 mM)-reduced samples; i–iii are as for panel A. EPR instrument conditions were as for Figure 1, but spectra were normalized to a protein concentration of 75 mg mL^{-1}. Reduced spectra were recorded at a gain 2.5× that used for the oxidized spectra.

the paramagnetic center is known. Meinhardt and Ohnishi (1992) compensated for differences between the T_1 values of different standards by using normalized $\Delta P_{1/2}$ values. This consideration is important in respect of our data, as there is a large difference between the intrinsic $P_{1/2}$ (and T_1) values of our distance standard (MbNO) and the DmsB-C102S [3Fe–4S] cluster. In our work the standard used is a soluble protein, whereas the DmsB-C102S [3Fe–4S] center is within the membrane extrinsic DmsAB dimer. It should be emphasized that the effective distance in these calculations is not the distance of the paramagnetic center below the DyEDTA-accessible surface but represents a weighted average distance over the entire surface. Also, the distance is based on assumptions about the topology of the DmsAB dimer, most importantly that the dimer is membrane extrinsic. We feel that this assumption is valid, as we have shown that [Fe–S] cluster containing soluble DmsAB dimer accumulates in the cytoplasm during growth of cells harboring the *dms* operon on a multicopy plasmid (Figure 8B; Sambasivarao et al., 1990; Cammack & Weiner, 1990). Also, electron microscopy data (Weiner et al., 1992) support a membrane extrinsic location for the DmsAB dimer. However, if we assume that the DmsAB dimer of the holoenzyme is buried in the membrane so that its probe-accessible surface is parallel to the membrane surface, then the distance becomes 29.5 Å (r^{-4} dependence). Thus the two extremes of topologies possible for the DmsAB dimer of the holoenzyme (membrane extrinsic and membrane intrinsic) yield distance estimates of 21 and 29.5 Å from the DmsAB dimer surface to the [3Fe–4S] center, respectively. However, we favor the 21-Å estimate, as this is based on reasonable assumptions about the topology of DmsABC.

Our results support a model for DMSO reductase in which the [4Fe–4S] cluster to which DmsB-C102S provides a ligand is located between the center of the membrane extrinsic DmsAB dimer and the DmsAB–DmsC interface region. The effective distance of the [3Fe–4S] cluster below the cytoplasmic surface of the protein is 21 Å, whereas the effective distance from the periplasmic surface is 42 Å (Table I). In cytoplasmic fractions containing DmsB-C102S soluble DmsAB dimer, the [3Fe–4S] cluster is not present (Figure 8), whereas the [4Fe–4S] clusters are present. This observation is consistent with the [3Fe–4S] cluster of the mutant protein being unstable due to its close proximity to the protein surface (i.e., the surface of the DmsAB dimer which interacts with DmsC in the holoenzyme). The [4Fe–4S] cluster ligated by C102 in wild-type DmsABC appears to be present in the wild-type soluble DmsAB dimer, as the line shape of its reduced spectrum appears to be identical to that of the spectrum of the enzyme in membrane samples. Given the importance of the [4Fe–4S] cluster to which DmsB-C102 provides a ligand in menaquinol:DMSO oxidoreductase activity, our results suggest that it is involved primarily in accepting electrons from menaquinol. The pathway of electrons through the four [4Fe–4S] clusters of the wild-type enzyme to the Moco cofactor of DmsA is not yet known, but site-directed mutagenesis studies are in progress to delineate it (R. A. Rothery and J. H. Weiner, work in progress). It will be very interesting to determine whether all of the clusters have electron transfer roles or whether one or more of them have primarily structural roles in defining the conformation of DmsB.

The topological data reported herein are relevant to the entire group of *E. coli* respiratory chain enzymes to which DMSO reductase belongs. These enzymes, NarGHJI, NarZYWV, and FdnGHI (Berg et al., 1991; Blasco et al., 1989, 1990), have a subunit composition similar to that of DMSO reductase. Comparisons with nitrate reductases, NarGHJI and NarZYWV, are particularly relevant (Cammack & Weiner, 1990; Rothery & Weiner, 1991). Guigliarelli et al. (1992) recently reported a detailed EPR study of these two nitrate reductases; the fully reduced spectra of these enzymes are spectrally similar to those reported herein [Figure 1(ii)] and elsewhere (Rothery & Weiner, 1991) for our DmsB-C102 mutants. The sequence and spectroscopic similarities between NarGHJI and NarZYWV suggest that the localization and function of the [3Fe–4S] cluster of nitrate reductase and the [4Fe–4S] cluster ligated by DmsB-C102 are similar. It would be interesting to test this hypothesis by carrying out a similar paramagnetic probe study of the *E. coli* nitrate reductases.

Overall, the data reported herein show that DmsB is located on the inside of the cytoplasmic membrane and that the DyEDTA probe technique can be applied to a protein containing a genetically engineered center. The sidedness data corroborate the findings of Sambasivarao et al. (1990) based on biochemical studies. In addition, we have been able to locate the position of the DmsB-C102S [3Fe–4S] cluster within the protein with low resolution and have shown that the position is consistent with the role of the corresponding

[4Fe–4S] cluster of the wild-type enzyme in electron transfer from menaquinol.

REFERENCES

Berg, B. L., Li, J., Heider, J., & Stewart, V. (1991) *J. Biol. Chem. 266*, 22380–22385.

Bilous, P. T., & Weiner, J. H. (1988) *J. Bacteriol. 170*, 1511–1518.

Bilous, P. T., Cole, S. T., Anderson, W. F., & Weiner, J. H. (1988) *Mol. Microbiol. 2*, 785–795.

Blasco, F., Iobbi, C., Giordano, G., Chippaux, M., & Bonnefoy, V. (1989) *Mol. Gen. Genet. 218*, 249–256.

Blasco, F., Iobbi, C., Ratouchniak, J., Bonnefoy, V., & Chippaux, M. (1990) *Mol. Gen. Genet. 222*, 104–111.

Blum, H., Leigh, J. S., & Ohnishi, T. (1980) *Biochim. Biophys. Acta 626*, 31–40.

Blum, H., Cusanovich, M. A., Sweeney, W. V., & Ohnishi, T. (1981) *J. Biol. Chem. 256*, 2199–2206.

Blum, H., Bowyer, J. R., Cusanovich, M. A., Waring, A. J., & Ohnishi, T. (1983) *Biochim. Biophys. Acta. 748*, 418–428.

Cammack, R., & Weiner, J. H. (1990) *Biochemistry 29*, 8410–8416.

Condon, C., & Weiner, J. H. (1988) *Mol. Microbiol. 2*, 43–52.

Guigliarelli, B., Asso, M., More, C., Augier, V., Blasco, F., Pommier, J., Giordano, G., & Bertrand, P. (1992) *Eur. J. Biochem. 207*, 61–68.

Hori, H., Ikeda-Saito, M., & Yonetani, T. (1981) *J. Biol. Chem. 256*, 7849–7855.

Innes, J. B., & Brudvig, G. W. (1989) *Biochemistry 28*, 1116–1125.

Lin, K., & Cheng, S. (1991) *Biotechniques 11*, 748–751.

Meinhardt, S. W., & Ohnishi, T. (1992) *Biochim. Biophys. Acta. 1100*, 67–74.

Nikaido, H., & Vaara, M. (1987) in *Escherichia coli and Salmonella typhimurium Cellular and Molecular Biology*, (Ingraham, J., Low, K. B., Magasanik, B., Schaetcher, M., Umbarger, H. E., & Neidhardt, F. C., Eds.) Vol. I, pp 7–22, American Society for Microbiology, Washington, D.C.

Ohnishi, T., Harmon, H. J., & Waring, A. J. (1985) *Biochem. Soc. Trans. 13*, 607–611.

Ohnishi, T., Schägger, H., Meinhardt, S. W., LoBrutto, R., Link, T. A., & von Jagow, G. (1989) *J. Biol. Chem. 264*, 735–744.

Rothery, R. A., & Weiner, J. H. (1991) *Biochemistry 30*, 8296–8305.

Rupp, H., Rao, K. K., Hall, D. O., & Cammack, R. (1978) *Biochim. Biophys. Acta. 537*, 255–269.

Sambasivarao, D., Scraba, D. G., Trieber, A., & Weiner, J. H. (1990) *J. Bacteriol. 172*, 5938–5948.

Trittelvitz, E., Sick, H., & Gersonde, K. (1972) *Eur. J. Biochem. 31*, 578–584.

Weiner, J. H., MacIsaac, D. P., Bishop, R. E., & Bilous, P. T. (1988) *J. Bacteriol. 170*, 1505–1510.

Weiner, J. H., Rothery, R. A., Sambasivarao, D., & Trieber, C. (1992) *Biochim. Biophys. Acta. 1102*, 1–18.